A&A manuscript no.
(will be inserted by hand later)

Your thesaurus codes are:
01 (03.01.1 08.03.4 08.09.2 08.14.2 13.09.6)

ASTRONOMY
AND
ASTROPHYSICS
4.9.1996

ISO observations of the classical nova V1974 Cygni *

A. Salama[1], A. Evans[2], S. P. S. Eyres[2], K. Leech[1], P. Barr[1], and M. F. Kessler[1]

[1] ISO Science Operations Centre, Astrophysics Division of ESA, Postbox 50727, E-28080 Villafranca/Madrid, Spain
[2] Department of Physics, Keele University, Keele, Staffordshire, ST5 5BG, U.K.

Received .... Accepted ....

Abstract. We present observations of the classical nova V1974 Cygni (Nova Cyg 1992) obtained with the ISO Short and Long Wavelength Spectrometers (SWS and LWS) and the spectrometer section of ISOPHOT. We identify [Ne III] λ15.5, [Ne V] λ14.3, 24.3, [Ne VI] λ7.6, [O III] λ51.8, [O IV] λ25.9. There is evidence that the Ne and O emission arises in physically distinct regions of the ejecta. We determine the electron temperatures in the Ne- and O-bearing regions of the ejecta, and estimate the Ne abundance relative to O.

Key words: circumstellar matter – Stars: individual: V1974 Cyg – novae, cataclysmic variables – Infrared: stars

1. Introduction

Classical nova eruptions arise following thermonuclear runaway on the surface of a white dwarf in a semi-detached binary system. Following the eruption, some $10^{-4}\,M_\odot$ of material, enriched in CNO, is ejected at $\sim 10^3\,\mathrm{km\,s^{-1}}$. In novae in which the white dwarf is a ONeMg white dwarf, the ejected material is also enriched in Ne, the so-called 'neon novae' (e.g. Starrfield 1990).

The classical nova V1974 Cyg (Nova Cygni 1992) was discovered on 1992 February 19. The early infrared (IR) evolution is described by Hayward et al. (1992, hereafter H92), Gehrz et al. (1994, G94) and Woodward et al. (1995, W95); optical and ultraviolet spectra are discussed in Austin et al. (1996; A96). Early IR spectra (H92, G94) showed, in addition to H recombination lines, strong [Ne II] λ12.8 and [Ne VI] λ7.6 emission. G94 and W95 estimated [Ne/Si] $\gtrsim 1$ for V1974 Cyg, while Paresce et al. (1995) derived a *conservative* lower limit $\mathrm{Ne/Ne}_\odot \sim 27$ (by mass), indicating that V1974 Cyg was a neon nova. In common with a number of novae (Greenhouse et al. 1990; G90), V1974 Cyg displayed a coronal phase (G94; A96).

We present here a preliminary account of the spectroscopic observations of V1974 Cyg carried out with ISO, which complement and extend the ground-based observations described by H92, G94, W95.

2. ISO observations

The observations were carried out on 1996 March 23 (day 1494 from outburst) using the short and long wavelength spectrometers (SWS and LWS) and the spectrometer mode of ISOPHOT; the observations were performed consecutively in time. Details are given in Table 1. We used the AOTs PHT-40, SWS-06 and LWS-01. These instrumental modes are described in Lemke et al. (1996), De Graauw et al. (1996) and Clegg et al. (1996) respectively. ISO as a whole is described in Kessler et al. (1996). In view of the fact that certain emission features (e.g. [C II] λ157) are ubiquitous in the interstellar medium (ISM) we also carried out a background observation with the LWS. In addition, we obtained broadband photometry with the AOTs PHT-03 and CAM-01; however these data are not presented here.

3. Results

3.1. ISOPHOT data

PHT-S data reduction was made by using the PHT Interactive Analysis, PIA V4.8, starting at the Edited Raw Data stage. Deglitching algorithms were applied to the detector ramps and to the signal. The baseline was determined and subtracted. The resulting PHT-S spectrum is shown in Fig. 1. There is a hint of a feature at $\sim 8.7\,\mu$m, which might correspond to [Na VI] λ8.6 (cf G94). However the only clearly identifiable feature is the [Ne VI] line at $7.6\,\mu$m, which was also present on day 264 (G94). We also note that, in contrast to the situation in 1992 (H92), the continuum is negligible; we can set an upper limit of 20 mJy in the $6 \ldots 8\,\mu$m wavelength range, compared with

Send offprint requests to: A. Salama

* The Infrared Space Observatory (ISO) is an ESA project with instruments funded by ESA Member States (especially the PI countries: France, Germany, the Netherlands and the United Kingdom) and with the participation of ISAS and NASA

Table 1. Observational details

Instrument	AOT	Wavelength range (μm)	UT Start	UT end	Details
PHT-S	PHT-40	2.5 - 5, 6 - 12	23-03-1996 06:08	06:27	Rectangular chop, 90″ throw
SWS	SWS-06	12 - 16.5, 19.5 - 29	23-03-1996 06:27	07:15	
LWS	LWS-01	43 - 196.6	23-03-1996 07:16	07:59	Spectral Sampling Interval 2, On-source
LWS	LWS-01	43 - 196.6	23-03-1996 08:00	08:21	Spectral Sampling Interval 2, Off-source

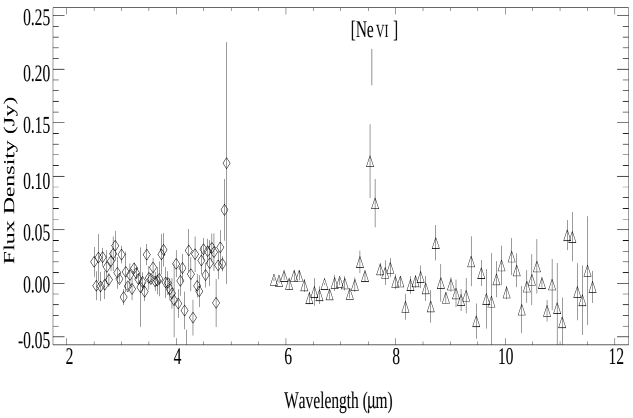

Fig. 1. PHT-S spectrum of V1974 Cyg. The higher noise level around 5 μm is due to high dark current of the two edge pixels of the PHT-S short-wavelength detector array.

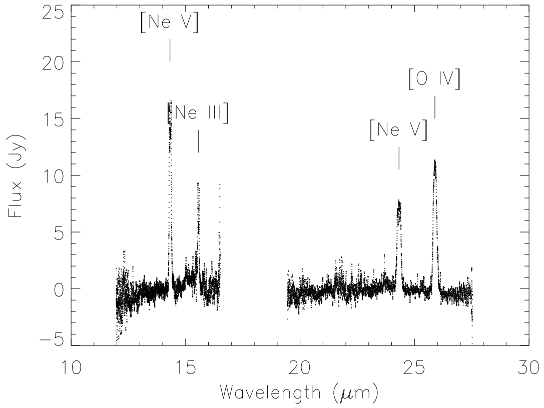

Fig. 2. The SWS spectrum of V1974 Cyg

$\sim$ 3.5 Jy at 12.8 μm in 1992. A simple extrapolation from 1992, assuming that the hydrogen density declines with time t as t^{-2} (appropriate for a shell expanding at constant thickness; see Paresce 1994, Paresce et al. 1995) and that the dimensions of the emitting region scale linearly with t, predicts that the free-free flux at the time of the ISO observations would have been $\lesssim$ 5 mJy, consistent with our upper limit.

3.2. SWS and LWS spectra

Reduction of LWS spectra was made running the processing pipeline V4.1. Reduction of SWS data was made within the Interactive Analysis environment using Calibration Files and pipeline modules as available at the time of writing, which is equivalent to processing the Edited Raw Data via the pipeline V4.3. The following additional processing steps were performed:

(i) Interpolation of dark currents as measured in the AOT SWS-06;
(ii) Elimination of detector 29 (much noisier than the others);
(iii) Flatfielding and 3-sigma clipping;
(iii) Rebinning to a resolution 1.5 times higher than the actual one, with oversample factor 8.

The SWS spectrum is shown in Fig. 2. The emission lines identified with PHT-S and SWS, together with their fluxes, are listed in Table 2; the quoted error bars are based on the absolute photometric accuracies as described in Schaeidt et al. (1996) for the SWS, in Swinyard et al. (1996) for the LWS, and Lemke et al. (1996) for PHT. The upper limits are 3σ.

Also listed are the critical electron densities (N_c) at which radiative de-excitation of the upper levels begins to dominate collisional de-excitation (Osterbrock 1989). [Ne II] λ12.8, which was strong during the early development of V1974 Cyg (H92, G94) was not securely detected by ISO. Furthermore, G94 predicted a number of forbidden sodium lines in the SWS wavelength range; we are not confident that we see any of these lines, to a flux limit of typically 10^{-19} W cm^{-2}.

There is considerable structure in the [Ne V] λ14.3, 24.3 lines (see Figs 3 and 4). Both lines may be fitted by four gaussians, corresponding to radial velocities -800 km s^{-1}, -200 km s^{-1}, 150 km s^{-1} and 600 km s^{-1}. The Hβ line profile in the months following outburst displayed radial velocities of $\sim$ -900 km s^{-1}, -500 km s^{-1}, -100 km s^{-1}, 400 km s^{-1} and 800 km s^{-1} (Chochol et al. 1993). The HWHM of these components correspond to velocities of 400 km s^{-1}, 200 km s^{-1}, 100 km s^{-1} and 500 km s^{-1} respectively. The FWHM of an SWS grating resolution element is 120 km s^{-1} at these wavelengths. In view of the close similarity of the [Ne V] line profiles (see Figs 3 and 4), we consider it unlikely that [Na VI] λ14.3 is contributing to the complexity of the [Ne V] λ14.3 line.

On the other hand, the [Ne III] λ15.5 line is fitted by only two gaussians, at -500 km s^{-1} and 400 km s^{-1} from the rest wavelength, with HWHM corresponding to ve-

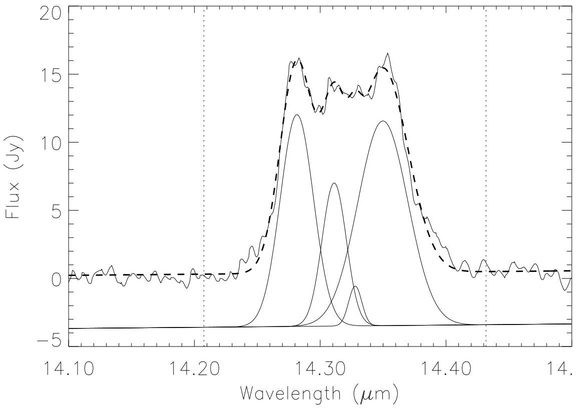

Fig. 3. Structure in the [Ne V] λ14.3 line. The dashed line is the fit to the underlying rebinned spectrum. Gaussian fitted components are shown below, shifted for clarity. Dotted lines indicate the range in which the baseline has been determined.

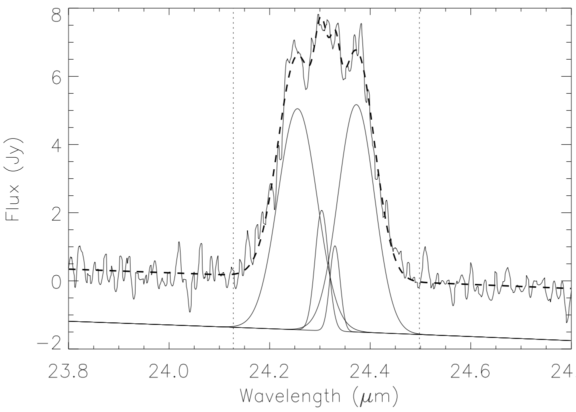

Fig. 4. Structure in the [Ne V] λ24.3 line.

Table 2. Emission line fluxes

λ (μm)	Ident	Transition	$N_c\,T^{-1/2}$	Flux
7.652	[Ne VI]	$^2P_{3/2}$ – $^2P_{1/2}$		1.0 ± 0.3
12.372	Hu-α	$7 \rightarrow 6$		< 6
12.814	[Ne II]	$^2P_{1/2}$ – $^2P_{3/2}$	$6.6\,10^3$	< 3
14.322	[Ne V]	$^3P_2$ – $^3P_1$	$3.8\,10^3$	25 ± 5
15.555	[Ne III]	$^3P_1$ – $^3P_2$	$1.8\,10^3$	4.6 ± 0.9
24.318	[Ne V]	$^3P_1$ – $^3P_0$	$1.8\,10^3$	7.5 ± 1.5
25.890	[O IV]	$^2P_{3/2}$ – $^2P_{1/2}$		8.7 ± 1.7
51.815	[O III]	$^3P_2$ – $^3P_1$	$3.8\,10^1$	4.4 ± 1.8
63.184	[O I]	$^3P_2$ – $^3P_1$	$5.2\,10^1$	< 0.5
88.356	[O III]	$^3P_1$ – $^3P_0$	$1.7\,10^1$	< 0.4
145.525	[O I]	$^3P_1$ – $^3P_0$		< 0.2
157.741	[C II]	$^2P_{3/2}$ – $^2P_{1/2}$	$8.5\,10^1$	< 0.6

The rest wavelengths of all neon lines and of the [O IV] λ25.9 line are from Feuchtgruber et al. (1996). The units for the quantities $N_c\,T^{-1/2}$ and Flux are (cm^{-3} K$^{-1/2}$) and (10^{-19} W cm^{-2}) respectively.

locities of 300 km s^{-1}. The fitting of a further two gaussians (as for the [Ne V] λ14.3, 24.3 lines) is not warranted in this case, although the line is strong enough for such structure, if present, to be resolvable. The structure of the [O IV] λ25.9 line is also relatively simple (see Fig. 5), consistent with a main gaussian component close to the rest wavelength, having a HWHM corresponding to a velocity of 900 km s^{-1} and a smaller component with a radial velocity of -800 km s^{-1} and a HWHM corresponding to a velocity of 350 km s^{-1}. The line profiles in novae often reflect the breaking up of the ejecta, into polar caps, and tropical and equatorial rings (e.g. Slavin, O'Brien & Dunlop 1995 and references therein). The Ne and O line profiles suggest that these species – and possibly even different ionization states of Ne – arise in different regions of the ejecta (cf. Evans et al. 1992).

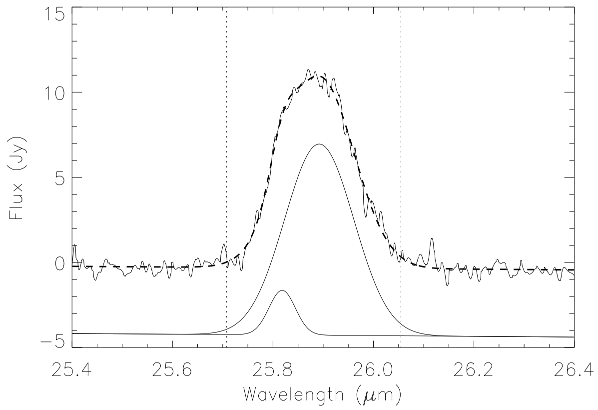

Fig. 5. Structure in the [O IV] λ25.9 line

In the LWS range we observe only the [O III] λ51.8 and [C II] λ157 lines, but the background observation shows that the latter originates entirely in the ISM.

4. Discussion

Extrapolation of the electron density N_e from 1992 would lead us to expect that $N_e \sim 10^5$ cm^{-3} in 1996. This is close to the expected critical density for a number of the lines in Table 2. If we consider the [Ne V] λ14.32, 24.32 lines, the flux ratio is

$$\frac{f(14.3)}{f(24.3)} = \frac{\lambda_{10}}{\lambda_{21}} \frac{\Omega_{20}}{\Omega_{10} + \Omega_{20}}, \qquad (N_e \ll N_c)$$
$$= \frac{\omega_1}{\omega_2} \frac{A_{21}}{A_{10}} \frac{\lambda_{10}}{\lambda_{21}} \qquad (N_e \gg N_c)$$

in the low and high density limits respectively. Here the λ_{ij} are the wavelengths of the ^3P_i–^3P_j transitions, the Ωs are the collision strengths, the ωs are the statistical weights of the upper levels and the As are the Einstein coefficients. For simplicity we have assumed that, in the low density limit, every collisional excitation leads to a radiative de-excitation, but we neglect the $^3P_2$–$^3P_0$ radiative transition (for which the transition probability is negligible by comparison with the transitions listed in Table 2) and the population of the ^{3}P level by cascades from the ^{1}S and ^{1}D levels. For $T_e \gtrsim 10^4$ K, the ratio $f(14.3)/f(24.3)$ is 0.57 in the low density limit and 10.2 in the high density limit. The observed ratio is 3.3, implying that the density is close to critical for the ^{3}P level of [Ne VI] and that, in fact, $N_e \simeq 1600\,T_e^{1/2}\,\mathrm{cm}^{-3}$ in the Ne-bearing region. If this density is also typical of the O-bearing region, then this would imply that the ^{3}P level of [O III] is in the high density regime, consistent with the non-detection of [O III] λ88.4 (see Table 2).

If we apply the prescription of G90 and the data in Jordan (1969) to the Ne lines to get an estimate of T_e in the Ne-bearing region, we find $T_e \simeq 10^{5.35\pm0.1}$ K; similarly the O lines can be used to estimate $T_e \simeq 10^{5.05\pm0.1}$ K – significantly lower than that in the Ne-bearing region – in the O-bearing region. These values of T_e are similar to those found by G90 in the coronal regions of other novae. However Austin et al. (1996) determined T_e in V1974 Cyg to be in the range $0.5\ldots2\times10^4$ K over the first few hundred days. Either T_e has increased over the intervening period, or the prescription of G90 is not applicable to this case. The latter is the more likely (cf. the discussion by Williams 1990), possibly because the G90 method implicitly neglects the radiation field.

The determination of T_e determines the electron density to be a few $\times10^5\,\mathrm{cm}^{-3}$, somewhat less than the critical densities for the Ne lines listed in Table 2. It is also consistent with extrapolation from 1992 (see above). If, as suggested by the line profiles, the Ne III and O IV emission arise in the same region we can use the Ne III/O IV ratio to estimate the abundance of Ne relative to O; we find that $N(\mathrm{Ne\,III})/N(\mathrm{O\,IV}) \simeq 2.9$. Using data in Jordan (1969) we find $N(\mathrm{O\,IV})/N(\mathrm{O}) = 0.27$ and $N(\mathrm{Ne\,III})/N(\mathrm{Ne}) = 0.85$, so that $N(\mathrm{Ne})/N(\mathrm{O}) \simeq 0.5$. This indicates that, in this region, Ne/O is $\simeq 4$ times the solar value. Austin et al. (1996) found this ratio to be 2.3; since the abundance determination is T_e–dependent the discrepancy may again be attributed to the fact that the prescription of G90 may not be appropriate. Nevertheless our results point to an overabundance of Ne relative to O. We are currently using CLOUDY90 (Ferland 1996) to model the emission line fluxes and the ISOPHOT photometry; the photometry and the results of this analysis will be reported elsewhere.

5. Concluding remarks

We have presented the first ISO observations of the classical nova V1974 Cyg. There is evidence that the Ne and O emission – and possibly even different ionization states of Ne – arise in different regions of the ejecta. The prescription of G90, if applicable, suggests electron temperatures of $10^{5.35}$ K and $10^{5.05}$ K in the Ne- and O-bearing regions respectively, although these may be overestimated; the electron density in the former region is a few $\times10^5\,\mathrm{cm}^{-3}$. We confirm that the ejecta are overabundant in Ne relative to O.

Acknowledgements. It is a pleasure to acknowledge the dedication of all colleagues involved with the ISO mission in general and the LIDT, PIDT and SIDT in particular. The award of time to observe novae with ISO within the SOC Guaranteed Time is also acknowledged. We thank Prof. J. Krautter for helpful comments on an earlier version of this paper. The ISOPHOT data presented in this paper were reduced using PIA, which is a joint development by the ESA Astrophysics Division and the ISOPHOT consortium led by the Max Planck Institute for Astronomy (MPIA), Heidelberg. SPSE is supported by the PPARC.

References

Austin, S. J., Wagner, R. M., Starrfield, S., et al., 1996, AJ, 111, 869 (A96)
Chochol, D., Hric, L., Urban, Z., et al., 1993, A&A, 277, 103
Clegg, P. E., et al., 1996, A&A, this issue
De Graauw, Th., et al., 1996, A&A, this issue
Evans, A., Bode, M. F., Duerbeck, H. W., Seitter, W. C., 1992, MNRAS, 258, 7P
Ferland, G, 1996, *HAZY*, University of Kentucky Department of Physics and Astronomy Internal Report
Feuchtgruber, H., Lutz, D., Beintema, D. A., et al., 1996, A&A, this issue
Gehrz, R. D., Woodward, C. E., Greenhouse, M. A., et al., 1994, ApJ, 421, 762 (G94)
Greenhouse, M. A., Grasdalen, G. L., Woodward, C. E., et al., 1990, ApJ, 352, 307 (G90)
Hayward, T. L., Gehrz, R. D., Miles, J. W., Houck, J. R., 1992, ApJ, 401, L101 (H92)
Jordan, C., 1969, MNRAS, 142, 501
Kessler, M. F., Steinz, J. A., Anderegg, M., et al., 1996, A&A, this issue
Lemke, D., Klaas, U., et al., 1996, A&A, this issue
Osterbrock, D. E., 1989, Astrophysics of Gaseous Nebulae and Active Galactic Nuclei, University Science Books
Paresce, F., 1994, A&A, 282, L13
Paresce, F., Livio, M., Hack, W., Korista, K., 1995, A&A, 299, 823
Schaeidt, S. G., Morris, P. W., Salama, A., Vandenbussche, B., et al., 1996, A&A, this issue
Slavin, A. J., O'Brien, T. J., Dunlop, J. S., 1995, MNRAS, 276, 353
Starrfield, S., 1990, in Physics of Classical Novae, Proceedings of IAU Colloquium 122, p.127, Eds A. Cassatella, R. Viotti, Springer-Verlag, Berlin
Swinyard, B. M., Clegg, P. E., et al., 1996, A&A, this issue
Williams, R. E., 1990, in Physics of Classical Novae, Proceedings of IAU Colloquium 122, p.215, Eds A. Cassatella, R. Viotti, Springer-Verlag, Berlin
Woodward, C. E., Greenhouse, M. A., Gehrz, R. D., et al., 1995, ApJ, 438, 921 (W95)

This article was processed by the author using Springer-Verlag LaTeX A&A style file *L-AA* version 3.